arXiv:1104.1679v1 [physics.plasm-ph] 9 Apr 2011

Cooling force on ions in a magnetized electron plasma

H.B. Nersisyan[*,a,b], G. Zwicknagel[b]

[a] *Division of Theoretical Physics, Institute of Radiophysics and Electronics, 0203 Ashtarak, Armenia*
[b] *Institut für Theoretische Physik II, Universität Erlangen-Nürnberg, Staudtstr. 7, D-91058 Erlangen, Germany*

Abstract

Electron cooling is a well–established method to improve the phase space quality of ion beams in storage rings. In the common rest frame of the ion and the electron beam the ion is subjected to a drag force and it experiences a loss or a gain of energy which eventually reduces the energy spread of the ion beam. A calculation of this process is complicated as the electron velocity distribution is anisotropic and the cooling process takes place in a magnetic field which guides the electrons. In this paper the cooling force is calculated in a model of binary collisions (BC) between ions and magnetized electrons, in which the Coulomb interaction is treated up to second order as a perturbation to the helical motion of the electrons. The calculations are done with the help of an improved BC theory which is uniformly valid for any strength of the magnetic field and where the second–order two–body forces are treated in the interaction in Fourier space without specifying the interaction potential. The cooling force is explicitly calculated for a regularized and screened potential which is both of finite range and less singular than the Coulomb interaction at the origin. Closed expressions are derived for monochromatic electron beams, which are folded with the velocity distributions of the electrons and ions. The resulting cooling force is evaluated for anisotropic Maxwell velocity distributions of the electrons and ions.

Key words: Cooling force, Energy loss, Electron cooler, Ion trap, Magnetized plasma

1. Introduction

In most experiments with particle beams a high phase space density is desired. In electron cooling of ion beams [1] this is achieved by mixing the ion beam with a comoving electron beam which has a very small longitudinal momentum spread. In the rest frame of the beams the cooling process may be viewed as the stopping of ions in an electron plasma [2–5]. More recently electron cooling has also been used in traps for precision experiments like CPT–tests with antihydrogen [6, 7] or planned QED–tests with highly charged ions in HITRAP [8]. In these applications the presence of strong external magnetic fields constitutes a theoretical challenge [9], as its influence on the cooling which the magnetized electrons exert on the ions (antiprotons) is not so obvious as earlier models might suggest. In the dielectric theory (DT) the drag on the ion is due to the polarization it creates in its wake. This can be either calculated in linear response (LR) [10, 11] or numerically by a particle–in–cell (PIC) simulation of the underlying nonlinear Vlasov–Poisson equation [12, 13]. While the LR requires cut–offs to exclude hard collisions of close particles the collectivity of the excitation can be taken into account in both approaches. In the complementary binary collision (BC) approximation the drag force is accumulated from the velocity transfers in individual collisions. This has been calculated by scattering statistical ensembles of magnetized electrons from the ions in the classical trajectory Monte–Carlo method (CTMC) [13–18], and by treating the Coulomb interaction as a perturbation to the helical motion of the electrons, see Refs. [19–25] for details. The observed cooling force $\mathbf{F}(\mathbf{v}_i)$ on an individual ion is obtained by integrating with respect to the impact parameter and the electrons velocity distribution. The ion velocity $\mathbf{v}_i$ is measured with respect to the center of that distribution. As in electron cooler the electrons are accelerated from the cathode, their velocity distribution is flattened longitudinally, but the spread does not vanish. As the cooling force

[*]Corresponding author
Email addresses: hrachya@irphe.am (H.B. Nersisyan), guenter.zwicknagel@physik.uni-erlangen.de (G. Zwicknagel)

on slow ions and therefore the cooling process depends critically on the details of the velocity distribution, a treatment employing a realistic velocity distribution is desirable.

The purpose of this paper is the application of a second order perturbative BC model for calculating the magnetized cooling force on a uniformly moving individual heavy ion as well as on a heavy ion beam. In previous approaches [19, 20] three regimes are identified, depending on the relative size of the cyclotron radius, the distance of the closest approach, and the pitch of the helix. The present paper is a continuation of our earlier studies in Refs. [21–25] where the second–order energy transfer for an electron–ion collision is calculated with the help of an improved BC treatment which unlike Ref. [19, 20] is valid for any strength of the magnetic field.

In Section 2 we introduce a perturbative binary collision formulation in terms of the binary force acting between the ion and a magnetized electron, and derive general expressions for the second–order (with respect to the interaction potential) cooling forces. These expressions involve all cyclotron harmonics of the electrons' helical motion, and are valid for any interaction potential and any strength of the magnetic field.

In Section 3 we turn to the explicit calculation of the second order cooling force without any restriction on the magnetic field in case of a regularized and screened interaction potential which is both of finite range and less singular than the Coulomb interaction at the origin and which includes as limiting cases the Debye (i.e., screened) and Coulomb potentials [26, 27]. In addition we calculate the magnetized cooling force averaged with respect to the electron and ion beams velocity distribution functions. The cooling force for monoenergetic electrons is folded with an anisotropic velocity distributions which is typical for electron cooling of ion beams in storage rings, where the velocity spread is much smaller longitudinal than transverse to the magnetic guiding field. A similar anisotropic distribution is used for averaging with respect to the ion velocity distribution. Also asymptotic expressions for large and small ion velocities and strong and vanishing magnetic fields are given.

Numerical results on the cooling force are presented in Section 4 using parameters of the ESR storage ring at GSI [28–30]. In particular, we compare our approach with the experimental data, the simplified treatment derived in Refs. [20, 25] and the model of Parkhomchuk [31].

2. Theoretical model

2.1. Binary collision (BC) formulation

We consider two point charges with masses m, M and charges $-e$, Ze, respectively, moving in a homogeneous magnetic field $\mathbf{B} = B\mathbf{b}$. We assume that the particles interact with the potential $-Z\ell^2 U(\mathbf{r})$ with $\ell^2 = e^2/4\pi\varepsilon_0$, where ε_0 is the permittivity of the vacuum and $\mathbf{r} = \mathbf{r}_1 - \mathbf{r}_2$ is the relative coordinate of the colliding particles. For two isolated charged particles this interaction is given by the Coulomb potential, i.e. $U_{\rm C}(\mathbf{r}) = 1/r$. In plasma applications the infinite range of this potential is modified by the screening. Then U may be modeled by $U_{\rm D}(\mathbf{r}) = e^{-r/\lambda}/r$ with a screening length λ, given e.g. by the Debye screening length $\lambda_{\rm D}$, see, for example [32]. The quantum uncertainty principle prevents particles (for $Z > 0$) from falling into the center of these potentials. In a classical picture this can be simulated by regularizing $U(\mathbf{r})$ at the origin, taking for example $U_{\rm R}(\mathbf{r}) = (1 - e^{-r/\lambda\!\!\!^{-}})e^{-r/\lambda}/r$, where $\lambda\!\!\!^{-}$ is usually related to the (thermal) de Broglie wavelength [26, 27]. Here, however, the use of this regularized interaction essentially represents an alternative implementation of the standard (lower) cutoff procedure needed to handle the hard collisions in a classical perturbative approach. Hence we consider $\lambda\!\!\!^{-}$ as a given constant or as a function of the classical collision diameter (see Section 4).

In the presence of an external magnetic field, the Lagrangian and the corresponding equations of particles motion cannot, in general, be separated into parts describing the relative motion and the motion of the center of mass (cm) [25]. However, in the case of heavy ions, i.e. $M \gg m$, the equations of motion can be simplified by treating the cm velocity $\mathbf{v}_{\rm cm}$ as a constant and equal to the ion velocity $\mathbf{v}_i$, i.e. $\mathbf{v}_{\rm cm} = \mathbf{v}_i = \text{const}$. Then the equation of relative motion turns into

$$\dot{\mathbf{v}}(t) + \omega_c \left[\mathbf{v}(t) \times \mathbf{b}\right] = -\omega_c \left[\mathbf{v}_i \times \mathbf{b}\right] - \frac{Z\ell^2}{m}\mathbf{f}\left(\mathbf{r}(t)\right), \tag{1}$$

where $\mathbf{v}(t) = \dot{\mathbf{r}}(t) = \mathbf{v}_e(t) - \mathbf{v}_i$ is the relative electron–ion velocity, $-Z\ell^2\mathbf{f}(\mathbf{r}(t))$ ($\mathbf{f} = -\partial U/\partial\mathbf{r}$) is the force exerted by the ion on the electron, $\omega_c = eB/m$ is the electron cyclotron frequency.

It is now useful to introduce the velocity correction through relations $\delta\mathbf{v}(t) = \mathbf{v}_e(t) - \mathbf{v}_{e0}(t) = \mathbf{v}(t) - \mathbf{v}_0(t)$, where $\mathbf{v}_{e0}(t)$ and $\mathbf{v}_0(t)$ are the unperturbed electron and relative velocities, respectively, with $\mathbf{v}_0(t) = \dot{\mathbf{r}}_0(t) = \mathbf{v}_{e0}(t) - \mathbf{v}_i$,

$$\mathbf{r}_0(t) = \mathbf{R}_0 + \mathbf{v}_r t + a\left[\mathbf{u}\sin(\omega_c t) - [\mathbf{b}\times\mathbf{u}]\cos(\omega_c t)\right], \tag{2}$$

$$\delta\dot{\mathbf{v}}(t) + \omega_c\left[\delta\mathbf{v}(t)\times\mathbf{b}\right] = -\frac{Z\ell^2}{m}\mathbf{f}(\mathbf{r}(t)) \tag{3}$$

and $\delta\mathbf{v}(t) \to 0$ at $t \to -\infty$. In Eq. (2) $\mathbf{u} = (\cos\varphi, \sin\varphi)$ is the unit vector perpendicular to the magnetic field, the angle φ is the initial phase of the electron's helical motion, $v_{e\|}$ and $v_{e\perp}$ (with $v_{e\perp} \geqslant 0$) are the unperturbed components of the electron velocity parallel and perpendicular to $\mathbf{b}$, respectively, $\mathbf{v}_r = v_{e\|}\mathbf{b} - \mathbf{v}_i$ is the relative velocity of the guiding center of the electrons, and $a = v_{e\perp}/\omega_c$ is the cyclotron radius. In Eq. (2), the variables $\mathbf{u}$ and $\mathbf{R}_0$ are independent and are defined by the initial conditions. In Eq. (3) $\mathbf{r}(t) = \mathbf{r}_e(t) - \mathbf{v}_i t$ is the ion–electron relative coordinate. We also introduce the variable $\mathbf{s} = \mathbf{R}_{0\perp} = \mathbf{R}_0 - \mathbf{n}_r(\mathbf{n}_r\cdot\mathbf{R}_0)$ which is the component of $\mathbf{R}_0$ perpendicular to the relative velocity vector $\mathbf{v}_r$ with $\mathbf{n}_r = \mathbf{v}_r/v_r$. From Eq. (2) we can see that $\mathbf{s}$ is the distance of closest approach between the ion and the guiding center of the electron's helical motion.

We seek an approximate solution of Eq. (3) in which the interaction force between the ion and electrons is considered as a perturbation. Thus we are looking for a solution of Eq. (3) for the variables $\mathbf{r}$ and $\mathbf{v}$ in a perturbative manner $\mathbf{r} = \mathbf{r}_0 + \mathbf{r}_1 + ...$, $\mathbf{v} = \mathbf{v}_0 + \mathbf{v}_1 + ...$, where $\mathbf{r}_0(t), \mathbf{v}_0(t)$ are the unperturbed ion–electron relative coordinate and velocity, respectively, $\mathbf{r}_n(t), \mathbf{v}_n(t)$ $(n = 1, 2, ...)$ are the nth order perturbations of $\mathbf{r}(t)$ and $\mathbf{v}(t)$, which are proportional to Z^n.

The equation for the first–order velocity correction is obtained from Eq. (3) replacing on the rhs the exact relative coordinate $\mathbf{r}(t)$ by $\mathbf{r}_0(t)$ with the solutions $\mathbf{v}_1(t) = \dot{\mathbf{r}}_1(t)$ and

$$\mathbf{r}_1(t) = \frac{Z\ell^2}{m}\left\{-\mathbf{b}P_\|(t) + \mathrm{Re}\left[\mathbf{b}\left(\mathbf{b}\cdot\mathbf{P}_\perp(t)\right) - \mathbf{P}_\perp(t) + i\left[\mathbf{b}\times\mathbf{P}_\perp(t)\right]\right]\right\}. \tag{4}$$

Here we have introduced the following abbreviations

$$P_\|(t) = \int_{-\infty}^{t}\mathbf{b}\cdot\mathbf{f}(\mathbf{r}_0(\tau))(t-\tau)\,d\tau, \quad \mathbf{P}_\perp(t) = \frac{1}{i\omega_c}\int_{-\infty}^{t}\mathbf{f}(\mathbf{r}_0(\tau))\left[e^{i\omega_c(t-\tau)} - 1\right]d\tau \tag{5}$$

and have assumed that all corrections vanish at $t \to -\infty$. As will be shown in the next Section, Eqs. (2) and (4) completely determine the second order cooling force on the ion.

2.2. Second order cooling forces

We now consider the interaction process of an individual ion with a homogeneous electron beam described by a velocity distribution function $f(\mathbf{v}_e)$ and a density n_e. We assume that the ion experiences independent binary collisions (BCs) with the electrons. The total cooling force acting on the ion is then obtained by multiplying the binary force $Z\ell^2\mathbf{f}(\mathbf{r}(t))$ by the element of the electron relative flux $n_e v_r d^2\mathbf{s}dt$ (where $\mathbf{s}$ is the impact parameter introduced above which is perpendicular to the relative velocity $\mathbf{v}_r$) and integrating with respect to time and folding with velocity distribution of the electrons. The result reads

$$\mathbf{F}(\mathbf{v}_i) = Z\ell^2 n_e\int d\mathbf{v}_e f(\mathbf{v}_e) v_r\int d^2\mathbf{s}\int_{-\infty}^{\infty}\mathbf{f}(\mathbf{r}(t))\,dt \tag{6}$$

and is an exact relation for uncorrelated BCs of the ion with electrons. We evaluate this expression within a systematic perturbative treatment considering only the second order force $\mathbf{F}_2$ with respect to the binary interaction since the averaged first order force $\mathbf{F}_1$ vanishes due to symmetry reasons [21–25]. Within the second order perturbation treatment the cooling force can be represented as:

$$\mathbf{F}_2 = Z\ell^2 n_e\int d\mathbf{v}_e f(\mathbf{v}_e) v_r\int d^2\mathbf{s}\int d\mathbf{k}U(\mathbf{k})\,\mathbf{k}\int_{-\infty}^{\infty}\left[\mathbf{k}\cdot\mathbf{r}_1(t)\right]e^{i\mathbf{k}\cdot\mathbf{r}_0(t)}dt. \tag{7}$$

Here we have introduced the two-particle interaction potential $U(\mathbf{r})$ and the binary force $\mathbf{f}(\mathbf{r})$ has been written using Fourier transformation in space. Furthermore the factor $e^{i\mathbf{k}\cdot\mathbf{r}(t)}$ in the Fourier transformed binary force has been

expanded in a perturbative manner as $e^{i\mathbf{k}\cdot\mathbf{r}(t)} \simeq e^{i\mathbf{k}\cdot\mathbf{r}_0(t)}[1 + i\mathbf{k}\cdot\mathbf{r}_1(t)]$, where $\mathbf{r}_0(t)$ and $\mathbf{r}_1(t)$ are the unperturbed and the first order corrected relative coordinate, Eqs. (2) and (4), respectively, e.i.

$$\mathbf{f}(\mathbf{r}(t)) = -i\int d\mathbf{k}U(\mathbf{k})\,\mathbf{k}\,e^{i\mathbf{k}\cdot\mathbf{r}(t)} \simeq -i\int d\mathbf{k}U(\mathbf{k})\,\mathbf{k}\,[1 + i\mathbf{k}\cdot\mathbf{r}_1(t)]\,e^{i\mathbf{k}\cdot\mathbf{r}_0(t)}. \tag{8}$$

From Eq. (7) it is seen that the second order cooling force, $\mathbf{F}_2$, is proportional to Z^2.

Substituting Eqs. (4) and (5) into Eq. (7) and writing the binary force in expression (5) in terms of Fourier transformed potential results in

$$\mathbf{F}_2 = \frac{iZ^2\not{e}^4 n_e}{m}\int d\mathbf{v}_e f(\mathbf{v}_e)\,v_r\int d^2\mathbf{s}\int d\mathbf{k}d\mathbf{k}'U(\mathbf{k})\,U(\mathbf{k}')\,\mathbf{k}\int_{-\infty}^{\infty}e^{i\mathbf{k}\cdot\mathbf{r}_0(t)}dt\int_{-\infty}^{t}e^{i\mathbf{k}'\cdot\mathbf{r}_0(\tau)}d\tau \tag{9}$$
$$\times\left\{g_0(t-\tau) + \frac{g_1}{\omega_c}\sin(\omega_c(t-\tau)) - \frac{g_2}{\omega_c}[1-\cos(\omega_c(t-\tau))]\right\},$$

where $g_0 = (\mathbf{k}\cdot\mathbf{b})(\mathbf{k}'\cdot\mathbf{b})$, $g_1 = (\mathbf{k}\cdot\mathbf{k}') - (\mathbf{k}\cdot\mathbf{b})(\mathbf{k}'\cdot\mathbf{b})$, $g_2 = (\mathbf{k}\cdot[\mathbf{k}'\times\mathbf{b}])$. The time-integral in Eq. (9) can be performed using the Fourier series expansion of the exponential function $e^{i\mathbf{k}\cdot\mathbf{r}_0(t)}$ with Eq. (2) (see, e.g., Ref. [33]). This yields

$$\mathbf{F}_2 = \frac{2\pi iZ^2\not{e}^4 n_e}{m}\int d\mathbf{v}_e f(\mathbf{v}_e)\,v_r\int d^2\mathbf{s}\int d\mathbf{k}d\mathbf{k}'U(\mathbf{k})\,U(\mathbf{k}')\,\mathbf{k}e^{i(\mathbf{k}+\mathbf{k}')\cdot\mathbf{R}_0}$$
$$\times\sum_{n,m=-\infty}^{\infty}e^{i(n+m)\varphi}e^{-in\theta-im\theta'}J_n(k_\perp a)\,J_m(k'_\perp a)\,\delta(\zeta_n(\mathbf{k}) + \zeta_m(\mathbf{k}')) \tag{10}$$
$$\times\left\{-\frac{g_0}{[\zeta_m(\mathbf{k}') - i0]^2} + \frac{g_1}{2\omega_c}\left[\frac{1}{\zeta_{m+1}(\mathbf{k}') - i0} - \frac{1}{\zeta_{m-1}(\mathbf{k}') - i0}\right]\right.$$
$$\left. + \frac{ig_2}{2\omega_c}\left[\frac{2}{\zeta_m(\mathbf{k}') - i0} - \frac{1}{\zeta_{m+1}(\mathbf{k}') - i0} - \frac{1}{\zeta_{m-1}(\mathbf{k}') - i0}\right]\right\}.$$

Here J_n are the Bessel functions of the nth order, $\tan\theta = k_y/k_x$, $k_\parallel = (\mathbf{k}\cdot\mathbf{b})$ and $k_\perp$ are the components of $\mathbf{k}$ parallel and transverse to $\mathbf{b}$, respectively, $\zeta_n(\mathbf{k}) = n\omega_c + \mathbf{k}\cdot\mathbf{v}_r$, and φ is the initial phase of the electron as defined in the previous Section. Note that expression (10) involves all cyclotron harmonics.

Next, we integrate with respect to the initial phase φ and impact parameter $\mathbf{s}$. For that purpose we recall that the volume element $d\mathbf{v}_e$ can be represented in cylindrical coordinates as $d\mathbf{v}_e = dv_{e\parallel}v_{e\perp}dv_{e\perp}d\varphi$, where $v_{e\parallel}$ and $v_{e\perp}$ are the electron velocity components parallel and transverse to $\mathbf{b}$, respectively. The $\mathbf{s}$–integration is enabled by using the relation $e^{i\mathbf{k}\cdot\mathbf{R}_0} = e^{i\kappa_\parallel R_{0\parallel}}e^{i\boldsymbol{\kappa}_\perp\cdot\mathbf{s}}$, where $\kappa_\parallel = \mathbf{k}\cdot\mathbf{n}_r$, $\boldsymbol{\kappa}_\perp = \mathbf{k} - \mathbf{n}_r(\mathbf{k}\cdot\mathbf{n}_r)$, i.e. the component of $\mathbf{k}$ parallel and transverse to $\mathbf{n}_r$. Performing now the φ and $\mathbf{s}$–integrations results in

$$\mathbf{F}_2 = -\frac{(2\pi)^5 Z^2\not{e}^4 n_e}{2m}\int_{-\infty}^{\infty}dv_{e\parallel}\int_0^{\infty}f(v_{e\parallel}, v_{e\perp})\,v_{e\perp}dv_{e\perp}\int d\mathbf{k}\,|U(\mathbf{k})|^2\,\mathbf{k} \tag{11}$$
$$\times\sum_{n=-\infty}^{\infty}J_n^2(k_\perp a)\left\{k_\parallel^2\delta'(\zeta_n(\mathbf{k})) + \frac{k_\perp^2}{2\omega_c}[\delta(\zeta_{n+1}(\mathbf{k})) - \delta(\zeta_{n-1}(\mathbf{k}))]\right\},$$

where the prime indicates the derivative with respect to the argument. For deriving Eq. (11) we assumed an axially symmetric velocity distribution $f(\mathbf{v}_e) = f(v_{e\parallel}, v_{e\perp})$ and used $\delta(\kappa_\parallel)\delta(\boldsymbol{\kappa}_\perp) = \delta(\mathbf{k})$.

The n–summation in Eq. (11) can be done using the summation formula for $\sum_n e^{in\varphi}J_n^2(z)$, see Ref. [33]. We then obtain

$$\mathbf{F}_2 = \frac{(2\pi)^4 Z^2\not{e}^4 n_e}{m}\int_{-\infty}^{\infty}dv_{e\parallel}\int_0^{\infty}f(v_{e\parallel}, v_{e\perp})\,v_{e\perp}dv_{e\perp}\int d\mathbf{k}\,|U(\mathbf{k})|^2\,\mathbf{k} \tag{12}$$
$$\times\int_0^{\infty}\left[k_\parallel^2 + k_\perp^2\frac{\sin(\omega_c t)}{\omega_c t}\right]J_0\left(2k_\perp a\sin\frac{\omega_c t}{2}\right)\sin(\mathbf{k}\cdot\mathbf{v}_r t)\,tdt.$$

This is a general expression for the magnetized cooling force acting on an individual ion. It has been derived within second order perturbation theory but without any restriction on the strength of the magnetic field B.

Some limiting cases can be easily extracted from Eq. (12). For instance, at vanishing magnetic field $\sin(\omega_c t)/(\omega_c t) \to 1$ and the argument of the Bessel function should be replaced by $k_\perp v_{e\perp} t$. In the presence of an infinitely strong magnetic field, however, the term in Eq. (12) proportional to $k_\perp^2$ and the argument of the Bessel function vanish since the cyclotron radius $a \to 0$.

3. Cooling force for a regularized and screened Coulomb potential

In electron cooling of ion beams the velocity distribution of the electrons is anisotropic. It is usually modeled by a two–temperature anisotropic Maxwell distribution. As the ion beam had a radial position some mm off the electron beam axis in the experiments [28–30], an additional transverse cyclotron velocity v_c of the electrons has to be taken into account, see [30] for details. The velocity distribution relevant for the averaging in Eq. (12) is thus given by

$$f\left(v_{e\|}, v_{e\perp}\right) = \frac{1}{(2\pi)^{3/2} v_{\mathrm{th}\perp}^2 v_{\mathrm{th}\|}} e^{-v_{e\perp}^2/2v_{\mathrm{th}\perp}^2} e^{-(v_{e\|}-v_c)^2/2v_{\mathrm{th}\|}^2}, \tag{13}$$

where $v_c \simeq v_{\mathrm{th}\perp}$ in the present case and the thermal velocities are related to electron temperatures by $v_{\mathrm{th}\perp}^2 = T_\perp/m$, $v_{\mathrm{th}\|}^2 = T_\|/m$ (here the temperatures are measured in energy units). In this case the transversal ($\mathbf{F}_\perp = \mathbf{F} - \mathbf{b}F_\|$) and longitudinal ($F_\| = \mathbf{b}\cdot\mathbf{F}$) components of the cooling force (we drop here the index 2 for simplicity), Eqs. (12) and (13), after velocity integrations [33] can be represented in the forms

$$\left\{ \begin{array}{c} F_\perp(\mathbf{v}_i) \\ F_\|(\mathbf{v}_i) \end{array} \right\} = -\frac{8Z^2e^4n_e}{m\omega_c^2}\frac{(2\pi)^4}{4}\int_0^\infty dk_\| \int_0^\infty U^2(k)\, k_\perp dk_\perp \tag{14}$$
$$\times \int_0^\infty e^{-\frac{t^2}{2}k_\|^2 a_\|^2} e^{-k_\perp^2 a_\perp^2(1-\cos t)} \left(k_\|^2 + k_\perp^2 \frac{\sin t}{t}\right) \left\{ \begin{array}{c} k_\perp \cos\left(k_\| a_{i\|} t\right) J_1\left(k_\perp a_{i\perp} t\right) \\ k_\| \sin\left(k_\| a_{i\|} t\right) J_0\left(k_\perp a_{i\perp} t\right) \end{array} \right\} tdt$$

with $\mathbf{F}_\perp(\mathbf{v}_i) = \frac{\mathbf{v}_{i\perp}}{v_{i\perp}} F_\perp(\mathbf{v}_i)$. Here we have assumed a spherically symmetric potential $U(\mathbf{k}) = U(k)$ and have introduced the thermal cyclotron radii of the electrons $a_\perp = v_{\mathrm{th}\perp}/\omega_c$, $a_\| = v_{\mathrm{th}\|}/\omega_c$, and $a_{i\perp} = v_{i\perp}/\omega_c$, $a_{i\|} = \overline{v}_{i\|}/\omega_c$, $\overline{v}_{i\|} = v_{i\|} - v_c$. In general the cooling force is thus anisotropic with respect to the ion velocity $\mathbf{v}_i$.

For the Coulomb interaction $U(k) = U_{\mathrm{C}}(k)$, the full 2D integration over the $\mathbf{s}$–space results in a logarithmic divergence of the $\mathbf{k}$-integration in Eqs. (11) and (12). To cure this, cutoff parameters $k_{\min}$ and $k_{\max}$ must be introduced, see [22, 25] for details. Instead of doing so, we here employ the regularized screened potential $U(\mathbf{r}) = U_{\mathrm{R}}(r)$ introduced in Section 2.1 with the Fourier transformed

$$U_{\mathrm{R}}(k) = \frac{2}{(2\pi)^2}\left(\frac{1}{k^2+\lambda^{-2}} - \frac{1}{k^2+d^{-2}}\right), \tag{15}$$

where $d^{-1} = \lambda^{-1} + \lambda^{-1}$.

Up to now we have considered the magnetized cooling force acting on the individual ion which interacts with an electron beam with anisotropic velocity distribution. However, in some experiments the measured longitudinal cooling force represents an average over the drag forces on individual ions. For a comparison with our theoretical model the cooling force is thus interpreted as the average $\langle F_\|(\mathbf{v}_i)\rangle = \mathcal{F}$ of the component $F_\|(\mathbf{v}_i)$ of the drag force (14) parallel to the beam axis (and the magnetic field) over the ion distribution $f_i(v_{i\|}, v_{i\perp})$ in the beam (see, e.g., [34–36]), that is,

$$\mathcal{F} = 2\pi \int_{-\infty}^{\infty} dv_{i\|} \int_0^\infty f_i\left(v_{i\|}, v_{i\perp}\right) F_\|\left(v_{i\|}, v_{i\perp}\right) v_{i\perp} dv_{i\perp}. \tag{16}$$

Here we model the ion beam by the anisotropic Maxwell distribution

$$f_i\left(v_{i\|}, v_{i\perp}\right) = \frac{1}{(2\pi)^{3/2}\sigma_\perp^2\sigma_\|} e^{-v_{i\perp}^2/2\sigma_\perp^2} e^{-\left(v_{i\|}-\overline{v}_{i\|}\right)^2/2\sigma_\|^2}, \tag{17}$$

where $\sigma_\perp^2 = (1/2)\langle v_{i\perp}^2\rangle = T_{i\perp}/M$, $\sigma_\parallel^2 = \langle v_{i\parallel}^2\rangle - \widetilde{v}_{i\parallel}^2 = T_{i\parallel}/M$ with the effective transversal ($T_{i\perp}$) and longitudinal ($T_{i\parallel}$) temperatures of ions. Here M is the ion mass and $\widetilde{v}_{i\parallel}$ is the average cm velocity of the ion beam with respect to the electron beam.

This yields the averaged cooling force (16) by substituting Eqs. (14) and (17) into Eq. (16) and then integrating over $v_{i\perp}$ and $v_{i\parallel}$ as

$$\mathcal{F}(u) = -\frac{8Z^2\ell^4 n_e\lambda^2}{mv_{\mathrm{th}\parallel}^2}\frac{(2\pi)^4}{4}\int_0^\infty k_\parallel dk_\parallel \int_0^\infty U^2(k)\, k_\perp dk_\perp \tag{18}$$
$$\times \int_0^\infty e^{-\frac{t^2}{2}\left(k_\parallel^2\lambda^2\delta_\parallel^2 + k_\perp^2\lambda^2 D(t)\right)}\left(k_\parallel^2 + k_\perp^2\frac{\sin(\alpha t)}{\alpha t}\right)\sin\left(\sqrt{2}k_\parallel\lambda u t\right) t dt$$

with

$$D(t) = \delta^2 + \tau\left(\frac{2}{\alpha t}\sin\frac{\alpha t}{2}\right)^2. \tag{19}$$

The dimensionless parameters introduced in Eq. (18) are defined as $u = (\widetilde{v}_{i\parallel} - v_c)/\sqrt{2}v_{\mathrm{th}\parallel}$, $\alpha = \omega_c\lambda/v_{\mathrm{th}\parallel}$, $\delta_\parallel^2 = 1 + \sigma_\parallel^2/v_{\mathrm{th}\parallel}^2$, $\delta = \sigma_\perp/v_{\mathrm{th}\parallel}$, and $\tau = T_\perp/T_\parallel$ is the anisotropy parameter of the electron beam.

Finally substituting the interaction potential (15) into Eq. (18) and performing the $k_\parallel$–integration we arrive, after lengthly but straightforward calculations, at

$$-\mathcal{F}(u) = \frac{4\sqrt{\pi}Z^2\ell^4 n_e}{mv_{\mathrm{th}\parallel}^2} u\int_0^\infty \frac{dt}{t}\int_0^1 d\zeta\, \Phi(\psi(t,\zeta))\exp\left(-\frac{u^2\zeta^2}{P^2(\zeta)}\right)\frac{1-\zeta^2}{P^3(\zeta)\,Q(t,\zeta)} \tag{20}$$
$$\times\left[\frac{\zeta^2}{P^2(\zeta)}\left(3 - \frac{2u^2\zeta^2}{P^2(\zeta)}\right) + \frac{2\zeta^2}{Q(t,\zeta)}\frac{\sin(\alpha t)}{\alpha t}\right].$$

Here $P(\zeta) = (\delta_\parallel^2\zeta^2 + 1 - \zeta^2)^{1/2}$, $Q(t,\zeta) = D(t)\zeta^2 + 1 - \zeta^2$, $\psi(t,\zeta) = (t^2/2)(1-\zeta^2)/\zeta^2$,

$$\Phi(z) = e^{-z} + e^{-\varkappa^2 z} - \frac{2}{\varkappa^2 - 1}\frac{1}{z}\left(e^{-z} - e^{-\varkappa^2 z}\right), \tag{21}$$

where $\varkappa = \lambda/d = 1 + \lambda/\lambda$. Equation (20) is the main result of this paper. We next consider some limiting cases of this expression.

3.1. High-velocity and $B \to 0$ limit

In the high–velocity limit assuming $\widetilde{v}_{i\parallel} > (\omega_c\lambda, v_{\mathrm{th}\parallel;\perp}, \sigma_{\parallel;\perp})$ only small t contribute to the cooling force (20) due to the short time response of the electrons to the moving fast ions. In this limit we have $\sin(\alpha t)/\alpha t \to 1$ and $Q(t,\zeta) \to \delta_\perp^2\zeta^2 + 1 - \zeta^2$, where $\delta_\perp^2 = D(0) = \delta^2 + \tau$. The remaining t–integration can be performed explicitly (see Appendix A for details) and Eq. (20) turns into

$$-\mathcal{F}(u) \simeq \frac{8\sqrt{\pi}Z^2\ell^4 n_e}{mv_{\mathrm{th}\parallel}^2}\Lambda(\varkappa)\, u\int_0^1 \frac{\zeta^2 d\zeta}{[\delta_\parallel^2\zeta^2 + \delta_\perp^2(1-\zeta^2)]^{3/2}}\exp\left[-\frac{\zeta^2u^2}{\delta_\parallel^2\zeta^2 + \delta_\perp^2(1-\zeta^2)}\right]. \tag{22}$$

Here as in Refs. [22–25] we have also introduced the generalized Coulomb logarithm (see Appendix A)

$$\Lambda(\varkappa) = \frac{\varkappa^2+1}{\varkappa^2-1}\ln\varkappa - 1. \tag{23}$$

Note that Eq. (22) does not depend on the magnetic field, ω_c, as natural consequence of the short time response of the magnetized electrons and is also valid for vanishing magnetic field.

A further increase of the ion beam velocity yields

$$-\mathcal{F}(u) \simeq \frac{2\pi Z^2\ell^4 n_e}{mv_{\mathrm{th}\parallel}^2}\Lambda(\varkappa)\frac{1}{u^2}\left[\mathrm{erf}\left(\frac{u}{\delta_\perp}\right) - \frac{2}{\sqrt{\pi}}\frac{u}{\delta_\perp}e^{-u^2/\delta_\perp^2}\right] \tag{24}$$
$$\simeq \frac{2\pi Z^2\ell^4 n_e}{mv_{\mathrm{th}\parallel}^2}\frac{\Lambda(\varkappa)}{u^2},$$

i.e. the force decreases as $\mathcal{F}(u) \sim u^{-2}$ with the beam velocity. Here $\mathrm{erf}(z)$ is the error function.

3.2. Strong magnetic field

In the limit of very strong magnetic fields with $\omega_c\lambda \gg (\widetilde{v}_{i\|}, v_{\mathrm{th}\|;\perp}, \sigma_{\|;\perp})$ assuming that $\sin(\alpha t)/\alpha t \to 0$ and $Q(t,\zeta) \to \delta^2\zeta^2 + 1 - \zeta^2$ from Eq. (20) after lengthly but straightforward calculations we obtain

$$-\mathcal{F}(u) = \frac{8\sqrt{\pi}Z^2\ell^4 n_e}{mv_{\mathrm{th}\|}^2}\Lambda(\varkappa)\, u \int_0^1 \frac{\zeta^4 d\zeta}{[\delta_\|^2\zeta^2 + \delta^2(1-\zeta^2)]^{3/2}} \exp\left[-\frac{u^2\zeta^2}{\delta_\|^2\zeta^2 + \delta^2(1-\zeta^2)}\right]. \tag{25}$$

In particular, for the high–velocity limit with $\omega_c\lambda \gg u \gg 1$, Eq. (25) becomes

$$\begin{aligned} -\mathcal{F}(u) &\simeq \frac{3\pi Z^2\ell^4 n_e}{mv_{\mathrm{th}\|}^2}\Lambda(\varkappa)\frac{\delta^2}{u^4}\left[\mathrm{erf}\left(\frac{u}{\delta}\right) - \frac{2}{3\sqrt{\pi}}\frac{u}{\delta}\left(3 + \frac{2u^2}{\delta^2}\right)e^{-u^2/\delta^2}\right] \\ &\simeq \frac{3\pi Z^2\ell^4 n_e}{mv_{\mathrm{th}\|}^2}\Lambda(\varkappa)\frac{\delta^2}{u^4}. \end{aligned} \tag{26}$$

There is an important difference if we compare Eqs. (25) and (26) with Eqs. (22) and (24), respectively. The force (25) decays as $\mathcal{F}(u) \sim u^{-4}$ much faster than in Eq. (24). The velocity of the beam in Eq. (26) is large but is restricted to the value $\omega_c\lambda$, i.e. $1 \ll u \ll \omega_c\lambda$. Thus it cannot be arbitrary large. The velocity in Eqs. (22) and (24) is arbitrary large but now restricted below, $\widetilde{v}_{i\|} \gg \omega_c\lambda$, i.e. the magnetic field there cannot be arbitrary large.

Considering on the other hand also the case of small velocities $u \ll 1$ at strong magnetic fields, Eq. (25) becomes

$$-\mathcal{F}(u) \simeq \frac{8\sqrt{\pi}Z^2\ell^4 n_e}{5mv_{\mathrm{th}\|}^2\delta_\|\delta^2}\Lambda(\varkappa)\, uP\left(\frac{\delta_\|}{\delta}\right), \tag{27}$$

where

$$P(x) = \frac{5}{2(1-x^2)^2}\left[x^2 + 2 - \frac{3x}{\sqrt{|1-x^2|}}p(x)\right], \tag{28}$$

$$p(x) = \begin{cases} \arccos x & x < 1 \\ \ln(x + \sqrt{x^2-1}), & x > 1 \end{cases}. \tag{29}$$

As expected the low–velocity cooling force Eq. (27) strongly depends on the details of the distribution functions of electrons and ions.

More generally, a magnetic field is considered as strong, if the cyclotron radius a is smaller than the screening length λ of the effective interaction between the electrons and the ions. Then the drag is dominated by the contributions from the adiabatic collisions with $a < \lambda$. As the distance of closest approach is inversely proportional to the square of the relative velocity between the guiding center of the electron and the ion the influence of the magnetic field via adiabatic collisions tends to become more and more important for $v_i \to 0$.

3.3. Adjustment of the effective interaction

For application of our present results, which are obtained with the statical screened interaction $U_{\mathrm{R}}(r)$, to the electron cooling problem the static screening length λ has to be replaced by an appropriately chosen velocity–dependent, dynamical one. For a known average temperature $\overline{T} = \frac{1}{3}(T_\| + 2T_\perp)$ of the electrons with average thermal velocity $\overline{v}_{\mathrm{th}} = (\overline{T}/m)^{1/2}$ this can be done, for instance, by choosing the dynamical screening length $\lambda(\widetilde{v}_{i\|}) = \lambda_{\mathrm{D}}[1 + (\widetilde{v}_{i\|}/\overline{v}_{\mathrm{th}})^2]^{1/2}$, where λ_{D} is the averaged Debye radius $\lambda_{\mathrm{D}} = \overline{v}_{\mathrm{th}}/\omega_p$ and ω_p is the electron plasma frequency.

Next we have to specify the cutoff parameter $\lambda\!\!\!^{-}$ which is a measure of the softening of the interaction potential at short distances. As we discussed in the previous section the regularization of the potential (15) guarantees the existence of the s-integrations, but there remains the problem of treating hard collisions as accurate as possible. For a perturbation treatment the change in relative velocity of the particles must be small compared to v_r and this condition is increasingly difficult to fulfill in the regime $v_r \to 0$. This suggests to soften the potential near the origin the more the smaller v_r is. In fact the parameter $\lambda\!\!\!^{-}$ should be related to the de Broglie wavelength which is inversely proportional to v_r. Here, within a classical picture, we employ for the perturbative treatment a dynamical cutoff parameter $\varkappa(\widetilde{v}_{i\|}) = 1 + \lambda(\widetilde{v}_{i\|})/\lambda\!\!\!^{-}(\widetilde{v}_{i\|})$ [23, 24], where $\lambda\!\!\!^{-2}(\widetilde{v}_{i\|}) = Cb_0^2(\widetilde{v}_{i\|}) + \lambda\!\!\!^{-2}_0$ with $b_0(\widetilde{v}_{i\|}) = |Z|\ell^2/m(\widetilde{v}_{i\|}^2 + v_{i\perp}^2 + \overline{v}_{\mathrm{th}}^2)$, where

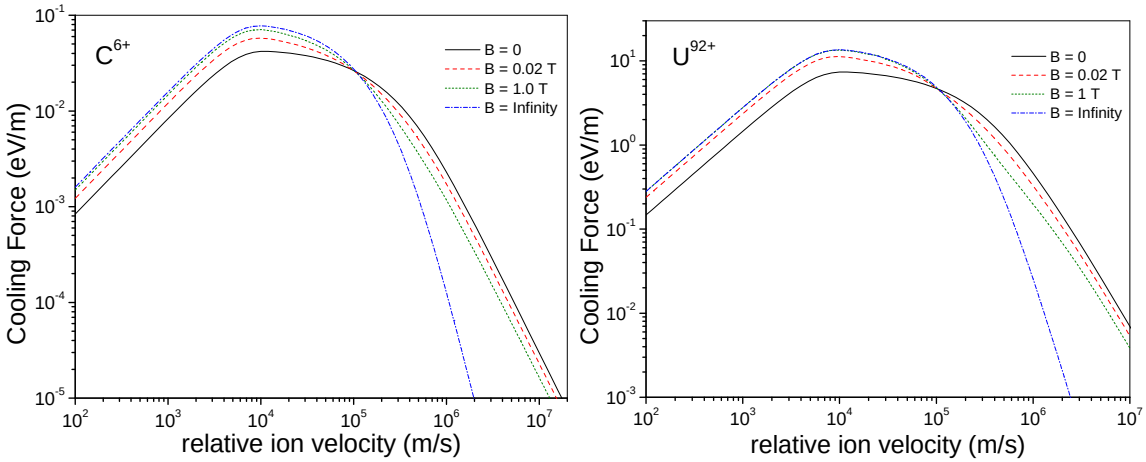

Figure 1: Longitudinal cooling force (in eV/m) for C^{6+} (left panel) and U^{92+} (right panel) fully stripped ions as function of the relative ion velocity (in m/s) with respect to the rest frame of the electron beam. The theoretical cooling force (20) is calculated for $\lambda\!\!\!^{-}_0 = 10^{-9}$ m and for an electron beam with $n_e = 10^6$ cm^{-3}, $T_\perp = 0.11$ eV and $T_\parallel = 0.1$ meV in a magnetic field of $B = 0$ (solid line), 0.02 T (dashed line), 1 T (dotted line), $B = \infty$ (dash–dotted line). The ion beam is characterized by the distribution $\sigma_\parallel = 0$, $\sigma_\perp = 3\langle v_{i\perp}\rangle$, $\theta_i = 0.2$ mrad (see the text for details).

$\lambda\!\!\!^{-}_0$ is some constant cutoff parameter, and b_0 is the averaged distance of closest approach of two charged particles in the absence of a magnetic field. Also in $\lambda\!\!\!^{-}(\widetilde{v}_{i\parallel})$ we have introduced a fitting parameter $C \simeq 0.292$. In Refs. [23, 24] this parameter is deduced from the comparison of the second order scattering cross sections with an exact asymptotic expression derived in Ref. [37] for the Yukawa–type (i.e., with $\lambda\!\!\!^{-} \to 0$) interaction potential. As has been shown in Refs. [23, 24] the second–order cross sections for electron–electron and electron–ion (with and without cyclotron gyration of the ion) collisions with dynamical cutoff parameter $\lambda\!\!\!^{-}(\widetilde{v}_{i\parallel})$ excellently agrees with CTMC simulations at high velocities. As a consequence, the generalized Coulomb logarithm $\Lambda(\varkappa)$ determined by Eq. (23) depends now on the ion beam velocity $\widetilde{v}_{i\parallel}$ and behaves at high–velocities as $\Lambda(\varkappa) \simeq \ln\varkappa - 1 \simeq \ln(\widetilde{v}_{i\parallel}/\omega_p\lambda\!\!\!^{-}_0) - 1$. This velocity dependent behavior of $\Lambda(\varkappa)$ must be taken into account when considering the asymptotic expressions (22) and (25).

4. Results and discussion

With the theoretical formalism presented so far, we now study the cooling forces on the ions resulting from our analytical approach, Eq. (20), and compare them with available experimental data. But before starting this, we first consider some general properties of Eq. (20), in particular, the effect of the magnetic field and of a variation of the ion and electron distributions on the cooling force. In Fig. 1 the forces are plotted vs ion beam relative velocity for different values of the magnetic field. The two limiting cases of vanishing ($B = 0$, solid lines) and infinitely strong ($B = \infty$, dash–dotted lines) magnetic fields are obtained from Eqs. (22) and (25), respectively. The density and the temperatures of the electron beam are the same as in the experiments at ESR storage ring [28–30] (see below for details). The parameters $\sigma_\parallel$ and $\sigma_\perp$ of the ion beam are given in units of the quantity $\langle v_{i\perp}\rangle$ introduced below and are typical for many electron cooling experiments (see, e.g., Refs. [3, 34–36]). It is seen that the magnetic field increases the cooling force $\mathcal{F}(u)$ at low velocities while reducing it at high–velocities. As expected the cooling force is more sensitive to the magnetic field at small u where a rather weak field with $B = 0.02$ T produces some deviations from the $B = 0$ regime. At high–velocities and at strong magnetic field ($B = 1$ T) the cooling force strongly deviates from the extreme case with $B = \infty$, which is, however, not accessible for the present experiments at storage rings. Also we would like to note that at very high–velocities the cooling force (20) systematically deviates from Eq. (22) which is the leading order term $\mathrm{O}(\widetilde{v}_{i\parallel}^{-2})$ of high–velocity expansion of Eq. (20). This is because at $u \gg 1$ the next term with $\mathrm{O}(\widetilde{v}_{i\parallel}^{-4})$ in high–velocity expansion of Eq. (20) is proportional to $(\omega_c\lambda\!\!\!^{-}v_{\mathrm{th}\parallel}/\widetilde{v}_{i\parallel}^2)^2$ and at high–velocities behaves as $(\omega_c/\omega_p)^2(v_{\mathrm{th}\parallel}/\widetilde{v}_{i\parallel})^2 \sim \mathrm{O}(\widetilde{v}_{i\parallel}^{-2})$ due to the dynamical screening introduced above. Thus, at $u \gg 1$ and at finite magnetic field Eq. (20) deviates systematically from the regime of vanishing magnetic field, Eq. (22).

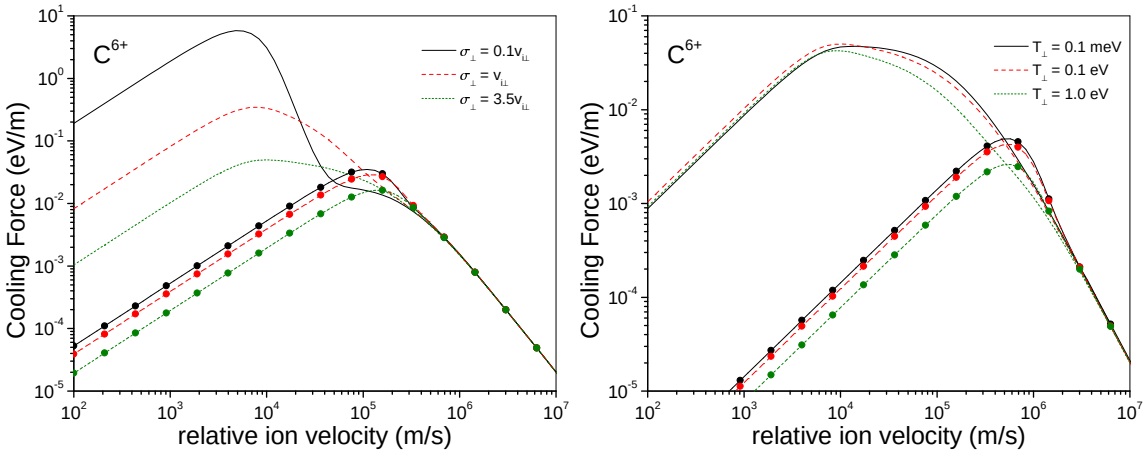

Figure 2: Same as in Fig. 1 for C^{6+} ions and for fixed magnetic field field with $B = 0.1$ T varying the shape of the distribution function of ions (left panel) and electrons (right panel). Left panel, $\sigma_\parallel = 0$, the lines without symbols and $\sigma_\parallel = 2\langle v_{i\perp}\rangle$, the lines with symbols. $\sigma_\perp = 0.1\langle v_{i\perp}\rangle$ (solid line), $\sigma_\perp = \langle v_{i\perp}\rangle$ (dashed line), $\sigma_\perp = 3.5\langle v_{i\perp}\rangle$ (dotted line). Right panel, $\sigma_\parallel = 0$, $\sigma_\perp = 3.5\langle v_{i\perp}\rangle$, $T_\parallel = 0.1$ meV, the lines without symbols and $T_\parallel = 1$ eV, the lines with symbols. $T_\perp = 0.1$ meV (solid line), $T_\perp = 0.1$ eV (dashed line), $T_\perp = 1$ eV (dotted line).

Next, in Fig. 2, the cooling forces on C^{6+} ions are plotted vs ion beam relative velocity for different shapes of the distribution functions of ions (left panel) and electrons (right panel). As expected at high–velocities the forces do not depend on the details of the distribution functions of the electron or ion beam. In the low–velocity regime $\mathcal{F}(u)$ is sensitive to both distributions showing, however, essential sensitivity to the transversal velocity spread of ions at small $\sigma_\parallel$, i.e., when the ion beam is nearly monochromatic in longitudinal direction (Fig. 2, left panel). As a general property of expression (20) we also mention the broadening of the profile of the cooling force at small $\sigma_\parallel$ with increasing the velocity spread $\sigma_\perp$ in transversal direction. Similarly, for a given ion beam (i.e. for a fixed $\sigma_{\parallel;\perp}$), the force profile is broadened with decreasing longitudinal energy spread $T_\parallel$ of the electrons.

Measurements of the cooling forces have been performed at several storage rings, like e.g. at the ESR at GSI [28–30]. In these experiments a so-called cooling force is extracted, which can be viewed as a stopping force averaged over the ion distribution in the beam and the electron distribution. As an example we focus on the measurements of longitudinal cooling forces for different fully stripped heavy ions as conducted at the electron cooler of the ESR storage ring. Two different methods have been used here to determine the cooling force. At low ion velocities the cooling force is extracted from the equilibrium between cooling and longitudinal heating with rf noise. At high relative velocities between the rest frames of the beams the cooling force is deduced from the momentum drift of the ion beam after a rapid change of the electron energy. Details of these methods are given in [28, 29]. The measured cooling forces are shown in Figs. 3 and 4 (filled circles).

The electron beam in these experiments has a density of $n_e \simeq 10^6$ cm^{-3} and can be described by an anisotropic velocity distribution (13) with $T_\perp = mv_{\text{th}\perp}^2 \simeq 0.11$ eV and $T_\parallel = mv_{\text{th}\parallel}^2 \simeq 0.1$ meV. As the ion beam had a radial position some mm off the electron beam axis in these experiments, an additional transverse cyclotron velocity v_c of the electrons has to be taken into account, see [30] for details. The velocity distribution relevant for the averaging in Eq. (12) is thus given by Eq. (13), where $v_c \simeq v_{\text{th}\perp}$ in the present case. The strength of the magnetic guiding field was $B = 0.1$ T. The measured longitudinal cooling force represents an average over the stopping forces on individual ions. For a comparison with the theoretical model (20) the cooling force is thus interpreted as the average $\langle F_\parallel\rangle$ of the component $F_\parallel$ of the stopping force (12) parallel to the beam axis (and the magnetic field) over the ion distribution $f_i(v_{i\parallel}, v_{i\perp})$ in the beam (see also [34–36]).

For low ion velocities this average is taken with respect to the transverse ion velocity only and the cooling force depends on the parallel ion velocity, i.e. $\langle F_\parallel\rangle = \langle F_\parallel\rangle(v_{i\parallel})$. In the experimental procedure used for high ion velocities the cooling force is an average over the complete ion distribution. This average $\langle F_\parallel\rangle = \langle F_\parallel\rangle(\langle v_{i\parallel}\rangle)$ depends now on the velocity of the cm of the ion beam relative to the rest frame of the electron beam $\langle v_{i\parallel}\rangle$. Both velocities are denoted as relative ion velocity in Figs. 3 and 4. To perform the average the distribution $f_i(v_{i\parallel}, v_{i\perp})$ must be known. However,

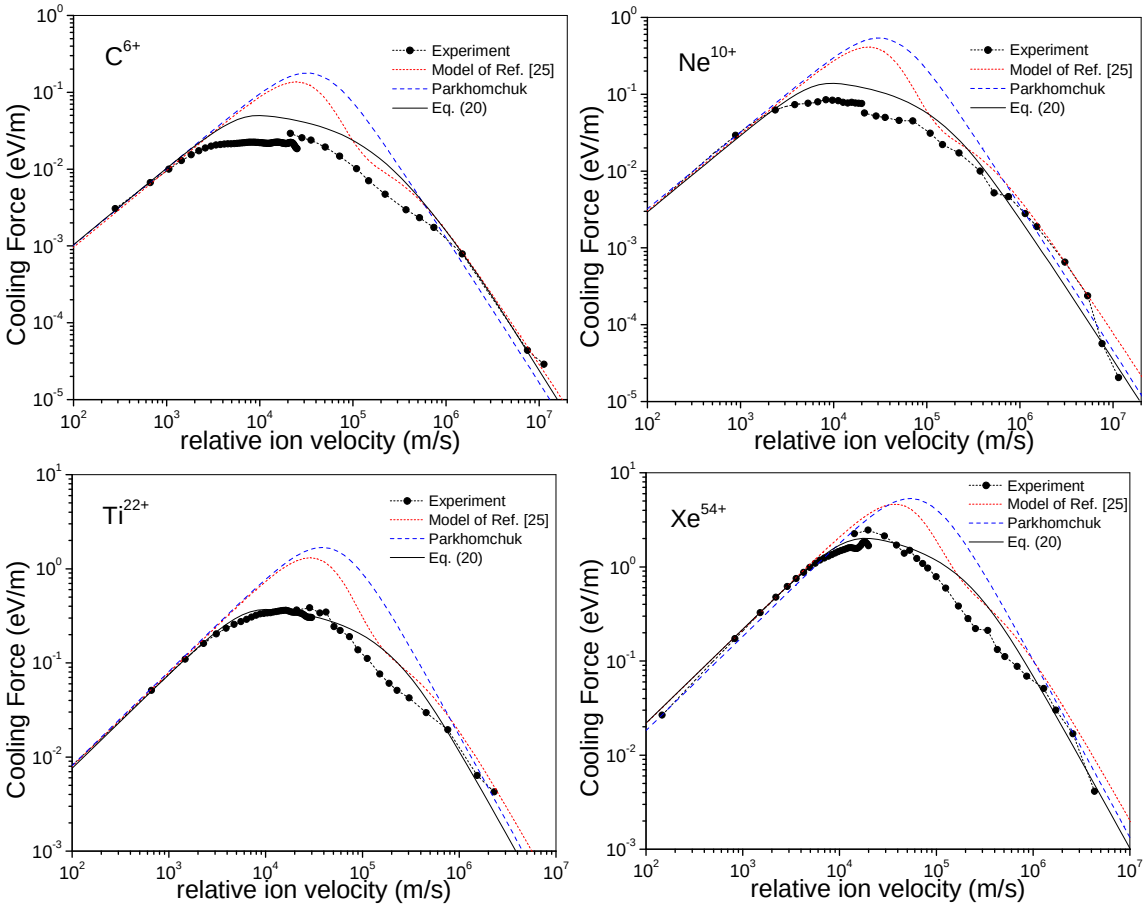

Figure 3: Longitudinal cooling force (in eV/m) for various fully stripped ions as function of the relative ion velocity (in m/s). Filled circles: experimental data from measurements at the electron cooler of the ESR storage ring [28–30]. Dotted curves: binary collision approximation proposed in [25]. Dashed curves: empiric formula (30) for the cooling force as proposed in [31]. Solid curves: equation (20). The theoretical descriptions of the cooling force are calculated for an electron beam with $n_e = 10^6$ cm^{-3}, $T_\perp = 0.11$ eV and $T_\parallel = 0.1$ meV in a magnetic field of $B = 0.1$ T, and are fitted to the experimental results at low relative velocities by treating the transverse ion velocity $\langle v_{i\perp}\rangle$ (for dotted and dashed curves) or the quantities $\sigma_{\parallel;\perp}$ (for solid curves) as a free parameter (see the text for details).

in Refs. [28–30] this distribution was not determined in detail, but there exists an estimate of the beam divergence $\langle\theta_i\rangle \lesssim 0.5$ mrad [29]. This yields after transformation to the rest frame of the ion beam for the transverse ion velocities $\langle v_{i\perp}\rangle \simeq \beta\gamma c\langle\theta_i\rangle$, where β, γ are the relativistic factors related to the beam velocity in the lab frame and c is the speed of light. For the measurements at hand with an ion energy of 250 MeV/u ($\beta = 0.615$, $\gamma = 1.268$) this results in $\langle v_{i\perp}\rangle \lesssim 10^5$ m/s.

In our previous simplified model [25] due to the lack of a more detailed knowledge about the ion distribution, the average with respect to $f_i(v_{i\parallel}, v_{i\perp})$ is replaced by $\langle F_\parallel\rangle = F_\parallel(v_{i\perp} = \langle v_{i\perp}\rangle, v_{i\parallel})$, where $v_{i\perp} = \langle v_{i\perp}\rangle$ was treated as a free parameter to fit the BC stopping force to the experimental data. As $F_\parallel(v_{i\perp}, v_{i\parallel})$ is rather sensitive to a variation of $v_{i\perp}$ at low parallel velocities $v_{i\parallel}$ this fit is done for the linear increase of the cooling force at low relative velocities. The related values for $v_{i\perp} = \langle v_{i\perp}\rangle$ are in the range $v_{i\perp}/v_{\mathrm{th}\parallel} = 10 - 17$ which corresponds to $\langle\theta_i\rangle \simeq 0.2 - 0.3$ mrad in good agreement with the estimated beam divergence. The resulting theoretical predictions are given by the dotted curves in Figs. 3 and 4. They agree well with the experimental data at low and high velocities but overestimate the cooling force at medium velocities $v_{\mathrm{th}\parallel} = 4.2 \times 10^3$ m/s $\lesssim v_{i\parallel} \lesssim v_{\mathrm{th}\perp} = 1.4 \times 10^5$ m/s.

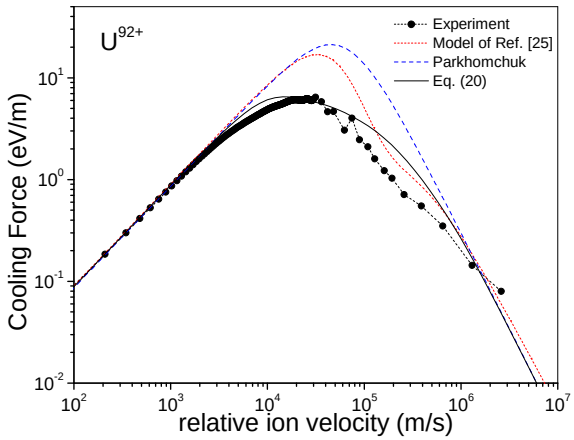

Figure 4: Same as in Fig. 3 but for U^{92+} ions.

The experimental data are also compared to an empirical formula for the cooling force

$$F_{\parallel}(\mathbf{v}_i) = -\frac{4\pi n_e Z^2 \not{e}^4}{m} \frac{v_{i\parallel}}{(v_{i\parallel}^2 + v_{i\perp}^2 + v_{\rm eff}^2)^{3/2}} \ln\left(1 + \frac{\langle s_{\rm max}\rangle}{\langle s_{\rm min}\rangle + a_\perp}\right) \tag{30}$$

as proposed by Parkhomchuk [31]. Here $\langle s_{\rm min}\rangle = Z\not{e}^2/m(v_i^2 + \overline{v}_{\rm th}^2)$ and $\langle s_{\rm max}\rangle = (v_i^2 + \overline{v}_{\rm th}^2)^{1/2}/\omega_p$ are the minimal and maximal impact parameters, $a_\perp = v_{{\rm th}\perp}/\omega_c$ is the cyclotron radius of the electrons, and $v_{\rm eff}$ is an effective electron velocity related to the transverse magnetic and electric fields in the electron cooler, see [31], which can be viewed as a fitting parameter. The force (30), which is the stopping force on a single ion, must also be averaged over the ion distribution like in (16). As above the force (30) with an average $\langle v_{i\perp}\rangle$ has been used instead. If the additional parameter is chosen as $v_{\rm eff} = v_{{\rm th}\parallel}$ (that is, rather small) the experimental data at low velocities are fitted by nearly the same values for the beam divergence $\langle\theta_i\rangle$ as before. The resulting cooling force is shown by the dashed curves in Figs. 3 and 4. The agreement with the experimentally deduced cooling force is as good as for the simplified BC force proposed in Ref. [25] (dotted curves) at low and high velocities. At medium velocities the deviation from the experimental results is even larger, in particular for $v_{i\parallel} \simeq v_{{\rm th}\perp}$, compared to the simplified but more detailed BC treatment of Ref. [25].

Now we turn to the present expression for the cooling force (20) which is shown as solid curves in Figs. 3 and 4 assuming the same beam divergence as in previous cases (i.e. $\langle\theta_i\rangle \simeq 0.2$ mrad). The velocity spread of the ion beam in transversal direction used in obtaining the solid curves is $3.5\beta\gamma c\langle\theta_i\rangle \lesssim \sigma_\perp \lesssim 4.5\beta\gamma c\langle\theta_i\rangle$ while the spread in the longitudinal direction is typically $\sigma_\parallel \lesssim 10^{-2}\sigma_\perp$ as it usually occurs in many experimental situations (see, e.g., [34–36] and references therein), in particular at ESR storage ring [28–30]. It is seen that the agreement of the more detailed Eq. (20) with the experimental cooling force is essentially improved in the whole relative velocity range compared to the simple models considered above (dotted and dashed curves). We mainly ascribe the deviations of the present model (solid curves) from the ESR data to the rather unknown distribution function of the ions in the beam which has been modeled here in the form of an anisotropic Maxwell distribution (17). Indeed the actual velocity spread in ion beams may essentially differ from the Maxwellian (17) and, in particular, in some cases the recorded profiles are parabolic rather than Maxwellian [34–36] (see also Ref. [3]). For a comprehensive comparison with the measurements and a critical evaluation of the theoretical approaches a detailed knowledge of the ion distribution is indispensable.

5. Summary

In this paper we have calculated the cooling force on ions in a model of binary collisions (BC) between ions and magnetized electrons within second order perturbative treatment. The calculations have been done with the help of an improved BC theory which is valid for any strength of the magnetic field. The cooling force is explicitly calculated

for a regularized and screened Coulomb potential. Closed expressions have been derived for monochromatic electron beams, which have been folded with the velocity distributions of the electrons and ions. The resulting cooling force is evaluated for anisotropic Maxwell velocity distributions of the electrons and ions. In addition, a number of limiting and asymptotic regimes of low– and high–velocities as well as vanishing and strong magnetic fields have been studied. The given results show that the present model of the cooling force is very sensitive to the velocity spreads of the electrons and ions at small relative velocities.

We have also compared our BC model with the previous theoretical approaches of Refs. [25, 31] as well as with the experiments performed at the ESR at GSI [28–30]. As demonstrated, the agreement of Eq. (20) with the experimental cooling forces considered over the whole relative velocity range is much better in comparison to the simplified BC model derived in Ref. [25] and Eq. (30) proposed by Parkhomchuk. The deviations of Eq. (20) from the ESR data, which can be seen in Figs. 3 and 4, are ascribed to the deviations of the model distribution function (17) from the experimental distribution of the ion beam which is not precisely known.

As the main goal of this paper we suggest a more advanced analytical model for calculations of the cooling force which is appropriate for modeling many experimental situations with moderate or strong magnetic guiding fields. In principle, the average involved in Eq. (16) can also be done numerically with recorded ion beam distributions or analytically using other ion distributions like e.g. the parabolic distribution function as it occurs in CELSIUS [35, 36]. Systematic comparisons for different distribution functions and other experiments on electron cooling as well as with Monte Carlo numerical simulations are currently in progress and the results will be reported elsewhere.

Finally we would like to mention that our results for the cooling forces $F_{\parallel}(\mathbf{v}_i)$ and $\mathcal{F}(u)$ can be tabulated in a suitable manner to be used as input for simulations of electron cooling using the BETACOOL package [38, 39].

Acknowledgements

One of the authors, H.B.N., is grateful for the support of the Alexander von Humboldt Foundation, Germany. This work was supported by the Bundesministerium für Bildung und Forschung (BMBF) under contract 06ER9064.

Appendix A. Derivation of the Coulomb logarithm

In this Appendix we evaluate briefly the t–integral remaining in Eq. (20) in the limit of high–velocity of the ion beam. This integral is given by

$$\int_0^\infty \frac{dt}{t}\Phi\left(\psi(t,\zeta)\right) = \frac{1}{2}\int_\varepsilon^\infty \frac{dz}{z}\Phi\left(z\right), \tag{A.1}$$

where $\varepsilon \to +0$ and the function $\Phi(z)$ is determined by Eq. (21). The second relation in Eq. (A.1) is obtained by introducing the new variable of integration $(t^2/2)(1/\zeta^2 - 1) = z$. Note that $\Phi(z) \sim z^2$ at $z \to 0$ and the second integral in Eq. (A.1) is convergent at vanishing z. However, we have introduced an infinitesimal $\varepsilon \to +0$ as the lower limit of integration which allows to perform separately z–integration of each term of the function $\Phi(z)$. The calculation is straightforward and the final result reads

$$\frac{\varkappa^2 + 1}{2(\varkappa^2 - 1)}[E_1(\varepsilon) - E_1(\varkappa^2\varepsilon)] - 1, \tag{A.2}$$

where $E_1(z)$ is the exponential integral. At small argument ($z \to 0$) this integral behaves as $E_1(z) \simeq \ln(1/z) - \gamma$ [33], where γ is Euler's constant. For $\varepsilon \to +0$, Eq. (A.2) thus turns into the generalized Coulomb logarithm $\Lambda(\varkappa)$ given by Eq. (23).

References

[1] G.I. Budker, Atomnaya Energiya **22** (1967) 346 [Sov. At. Energy **22** (1967) 438].
[2] A.H. Sørensen, E. Bonderup, Nucl. Instr. and Meth. **215** (1983) 27.
[3] H. Poth, Phys. Rep. **196** (1990) 135.
[4] I.N. Meshkov, Phys. Part. Nucl. **25** (1994) 631.
[5] L.I. Men'shikov, Physics–Uspekhi **51** (2008) 645.
[6] M. Amoretti, et al., Nature **419** (2002) 456.

[7] G. Gabrielse, et al., Phys. Rev. Lett. **89** (2002) 213401.
[8] W. Quint, et al., Hyperfine Interactions **132** (2001) 457.
[9] Ya.S. Derbenev, A.N. Skrinsky, Part. Accel. **8** (1978) 235.
[10] M. Walter (C. Toepffer, G. Zwicknagel advisors), thesis, University of Erlangen, 2002.
[11] H.B. Nersisyan, M. Walter, G. Zwicknagel, Phys. Rev. E **61** (2000) 7022.
[12] M. Walter, C. Toepffer, G. Zwicknagel, Nucl. Instr. and Meth. B **168** (2000) 347.
[13] B. Möllers, C. Toepffer, M. Walter, G. Zwicknagel, C. Carli, H.B. Nersisyan, Nucl. Instr. and Meth. A **532** (2004) 279.
[14] G. Zwicknagel, Theory and Simulation of the Interaction of Ions with Plasmas: Nonlinear Stopping, Ion-Ion Correlation Effects and Collisions of Ions with Magnetized Electrons, thesis, University of Erlangen, 2000. (`http://www.opus.ub.uni-erlangen.de/opus/volltexte/2008/913/`).
[15] G. Zwicknagel, in: J.B. Bollinger, R.L. Spencer, R.C. Davidson (Eds.), Non-Neutral Plasma Physics III, AIP Conference Proceedings, Vol. **498**, 1999, p. 469.
[16] G. Zwicknagel, C. Toepffer, in: F. Anderegg, L. Schweikhard, C.F. Driscoll (Eds.), Non-Neutral Plasma Physics IV, AIP Conference Proceedings, Vol. **606**, 2002, p. 499.
[17] G. Zwicknagel, in: S. Nagaitsev, R.J. Pasquinelli (Eds.), Beam Cooling and Related Topics, AIP Conference Proceedings, Vol. **821**, 2006, p. 513.
[18] G. Zwicknagel, Trapped Charged Particles and Fundamental Interactions, Lecture Notes in Physics Vol. 749, edited by K. Blaum and F. Herfurth, Springer-Verlag, Berlin, 2008, pp. 69-96.
[19] C. Toepffer, Phys. Rev. A **66** (2002) 022714.
[20] B. Möllers, M. Walter, G. Zwicknagel, C. Carli, C. Toepffer, Nucl. Instr. and Meth. B **207** (2003) 462.
[21] H.B. Nersisyan, Nucl. Instr. and Meth. B **205** (2003) 276.
[22] H.B. Nersisyan, G. Zwicknagel, C. Toepffer, Phys. Rev. E **67** (2003) 026411.
[23] H.B. Nersisyan, G. Zwicknagel, Phys. Rev. E **79** (2009) 066405.
[24] H.B. Nersisyan, G. Zwicknagel, Phys. Plasmas **17** (2010) 082314.
[25] H.B. Nersisyan, C. Toepffer, G. Zwicknagel, Interactions Between Charged Particles in a Magnetic Field: A Theoretical Approach to Ion Stopping in Magnetized Plasmas, Springer, Heidelberg, 2007.
[26] G. Kelbg, Ann. Physik **12** (1963) 219.
[27] C. Deutsch, Phys. Lett. A **60** (1977) 317.
[28] Th. Winkler et al., Hyperfine Int. **99** (1996) 277.
[29] Th. Winkler, Untersuchungen zur Elektronenkühlung hochgeladener schwerer Ionen, Thesis, University Heidelberg, Heidelberg (1996).
[30] Th. Winkler et al., Nucl. Instr. and Meth. A **391** (1997) 12.
[31] V.V. Parkhomchuk, Nucl. Instr. and Meth. A **441** (2000) 9.
[32] A.I. Akhiezer, I.A. Akhiezer, R.V. Polovin, A.G. Sitenko, K.N. Stepanov, Plasma Electrodynamics, 1st ed., vol. 1, Pergamon, Oxford, 1975.
[33] I.S. Gradshteyn, I.M. Ryzhik, Tables of Integrals, Series and Products, 2nd ed., Academic, New York, 1980.
[34] M. Beutelspacher, M. Grieser, K. Noda, and T. Shirai, Systematic investigation on electron cooling at the Heidelberg heavy ion storage ring. Proceedings of the Workshop on Ion Beam Cooling: Toward the Crystalline Beam (Kyoto, Japan, 12-14 November 2001), edited by A. Noda and T. Shirai, World Scientific, Singapore, 2002, pp. 93-128.
[35] A.V. Fedotov et al., in S. Nagaitsev, R.J. Pasquinelli (Eds.), Beam Cooling and Related Topics, AIP Conference Proceedings, Vol. **821**, 2006, p. 265.
[36] A.V. Fedotov et al., Phys. Rev. E **73** (2006) 066503.
[37] H. Hahn, E.A. Mason, F.J. Smith, Phys. Fluids **14** (1971) 278.
[38] A.Yu. Lavrentev, I.N. Meshkov, JINR preprint E9-95-317.
[39] N. Madsen, CERN/PS/DI/Note 99-20, AD Note 053 (1999).